American Mineralogist, Volume 84, pages 1650–1660, 1999

Khmaralite, a new beryllium-bearing mineral related to sapphirine: A superstructure resulting from partial ordering of Be, Al, and Si on tetrahedral sites

JACQUES BARBIER,[1,*] EDWARD S. GREW,[2] PAULUS B. MOORE,[3] AND SHU-CHUN SU[4]

[1]Department of Chemistry, McMaster University, Hamilton, Ontario, L8S 4M1 Canada
[2]Department of Geological Sciences, University of Maine 5790 Bryand Center
Orono, Maine 04469, U.S.A.
[3]P.O. Box 703, Warwick, New York,10990, U.S.A.
[4]Hercules Research Center, 500 Hercules Road, Wilmington, Delaware 19808, U.S.A.

ABSTRACT

Khmaralite, $Ca_{0.04}Mg_{5.46}Fe^{3+}_{0.12}Fe^{2+}_{1.87}Al_{14.26}Be_{1.43}B_{0.02}Si_{4.80}O_{40}$, is a new mineral closely related to sapphirine from Khmara Bay, Enderby Land, Antarctica. It occurs in a pegmatite metamorphosed at $T \geq 820$ °C, $P \geq 10$ kbar. The minerals surinamite, musgravite, and sillimanite associated with khmaralite at Casey Bay saturate it in BeO, and thus its BeO content could be close to the maximum possible. Optically, khmaralite is biaxial (–); at $\lambda = 589$ nm, $\alpha = 1.725(2)$, $\beta = 1.740(2)$, $\gamma = 1.741(2)$, $2V_{meas} = 34.4\ (1.8)°$, v > r strong, and $\beta \parallel b$. The weak superstructure reported using electron diffraction has been confirmed by single-crystal X-ray diffraction. The superstructure corresponds to a doubling of the **a** axis in monoclinic sapphirine-2*M* ($P2_1/c$ setting) with the following unit-cell parameters: $a = 19.800(1)$, $b = 14.371(1)$, $c = 11.254(1)$ Å, $\beta = 125.53(1)°$, $Z = 4$, $D_{calc} = 3.61$ g/cm^3. Using a simplified chemical formula of $Mg_{5.46}Al_{14.28}Fe_{2.00}Si_{4.80}Be_{1.46}O_{40}$, the fully anisotropic structure refinement of all site occupancies, including Al vs. Mg and Al vs. Si on the 16 octahedral (M) and 12 tetrahedral (T) sites respectively, establishes that the 2×**a** superstructure results primarily from ordering in the doubled (T1 → T6, T7 → T12) tetrahedral chain, which is parallel to the **a** axis. The strongest contribution comes from Al-Si-Be ordering on the T2 (33-16-51%) vs. T8 (0-95-5%) and T3 (4-78-18%) vs. T9 (30-0-70%) sites. Thus, the sequence Al-Si-Al in sapphirine is replaced by the sequence Si-Be-Si in khmaralite; i.e., Be replaces Si on two sites and Si replaces Al on on four adjacent sites, resulting in an indirect replacement of Al by Be by the coupled substitution Be + Si = 2Al. The Be distribution in khmaralite and the strong preference for Be/Al mixing over Be/Si mixing appear to satisfy the bonding requirements of the bridging O atoms by minimizing the number of Be-O-Be and Be-O-Al linkages.

INTRODUCTION

Sapphirine is one of the few rock-forming minerals which incorporates variable amounts of beryllium above the trace level; up to 0.65 wt% BeO has been measured (Wilson and Hudson 1967). However, Grew (1981) estimated that as much as 2.5 wt% BeO could be present in a sapphirine from Khmara Bay (67° 20' S; 49° 00' E), the easternmost extension of Casey Bay, Antarctica, an estimate confirmed by subsequent ion microprobe analyses. Using transmission electron microscopy, Christy (1988) reported a superstructure of sapphirine-2*M* with a doubled **a** axis repeat in the Khmara Bay sapphirine, which he attributed to Be-Si ordering: competition between Si and Be for the most polymerized sites in the tetrahedral chains. P.B. Moore (unpublished data) attempted to identify the superstructure with X-rays, but without success.

In this study, crystallographic refinement of the superstructure confirms the presence of significant Be-Si-Al ordering, but not in the scheme suggested by Christy (1988); instead significant Be (51–70%) is present on one of the two sites coordinated to three other tetrahedra in each of the sapphirine-like sub-cells. This phase is not "beryllosapphirine" because such a mineral should have the same space group as sapphirine-2*M* and similar cell parameters. We chose the name khmaralite from the locality Khmara Bay, which honors Ivan Fedorovich Khmara (1936–1956), a tractor driver on the Soviet Antarctic Expedition who perished in Antarctica. The new mineral and the name have been approved by the Commission on New Minerals and Mineral Names of the IMA. Holotype material is preserved in the National Museum of Natural History, Smithsonian Institution as NMNH 171532.

Sapphirine is structurally most closely related to the aenigmatite group, which includes the beryllosilicate minerals høgtuvaite, welshite and "makarochkinite," and to the ferromagnesian aluminum beryllosilicate mineral surinamite. No structure determination is presently available for either høgtuvaite, $(Ca,Na)_2(Fe,Ti,Mg,Mn,Sn)_6(Si,Be,Al)_6O_{20}$ (Grauch et al. 1994) or welshite, $Ca_2(Mg,Mn)_4FeSb(Si,Be,As,Al)_6O_{20}$ (Moore 1978). "Makarochkinite" (not approved by the IMA Commission on New Minerals and Mineral Names), $(Ca,Na)_2(Fe,Ti,Mg,Mn)_6(Si,Be,Al)_6O_{20}$ (Polyakov et al. 1986), is chemi-

*E-mail: barbier@mcmaster.ca

cally nearly identical to høgtuvaite (Grauch et al. 1994), but optical properties and the absence of polysynthetic twinning in "makarochkinite" suggest that the two minerals could be distinct species. Yakubovich et al. (1990) refined the structure of "makarochkinite" and reported unexpected Be/Si mixing on two of the tetrahedral sites. In the case of sapphirine, $(Mg,Al,Fe)_8(Al,Si)_6O_{20}$, structure determinations have been carried out for sapphirine-2*M* (Moore 1968, 1969; Higgins and Ribbe 1979b) and sapphirine-1*A* (Merlino 1980). None of these studies, including one which used single-crystal neutron diffraction to refine the octahedral Mg/Al and tetrahedral Al/Si occupancies (Higgins and Ribbe 1979b), reported the presence of a superstructure. A later study of natural and synthetic sapphirines by electron diffraction and microscopy did not detect any superstructure either (Christy and Putnis 1988). In the case of surinamite, $(Mg_3Al_3)(Si_3BeAl)O_{16}$, only one structure determination has been done (Moore and Araki 1983). The refinement of the octahedral Mg/Al distribution was not attempted but the tetrahedral Si/Be/Al distribution was found to be fully ordered. Beryllium has been shown to be essential for the stability of the surinamite phase in the Mg-Al-Si-Be-O system (de Roever et al. 1981; Hölscher et al. 1986) and its crystal chemical role may be linked to the tetrahedral ordering in the crystal structure. The structure of khmaralite described here represents another example of the role of beryllium in inducing tetrahedral ordering.

PETROGRAPHIC DESCRIPTION

Khmaralite was found in a single specimen of pegmatite, no. 2234L(3) from "Zircon Point" on Khmara Bay; a small grain of Si-rich sapphirine containing 1.7 wt% BeO, which could be khmaralite, is enclosed in garnet in a specimen from the same pegmatite, no. 2234L(2) (Grew 1981; Grew and Shearer, unpublished data). In no. 2234L(3), khmaralite forms a foliated aggregate nearly 3 cm across of parallel tablets in a pegmatite consisting largely of quartz and microcline. The tablets are flattened parallel to {010} and a few grains show these faces. Individual tablets range from 1 to 7 mm across and from 0.5 to 4 mm thick as seen in thin section. Khmaralite is most closely associated with sillimanite, surinamite, musgravite, garnet, and biotite, which are also major constituents of the aggregate; other associated minerals are apatite, rutile, and very sparse dumortierite. Spinel is found interstitial to sillimanite prisms at one spot and is isolated from khmaralite, which also has no contact with either quartz or microcline. Chrysoberyl is present in no. 2234L(2), but given the isolation of the possible khmaralite by garnet, there is no evidence that khmaralite is stable with chrysoberyl.

PETROGENESIS

The textures of the aggregates, particularly the relatively fine grain size (few mm to nearly 3 cm) and preferred orientation, suggest a metamorphic origin. Grew (1998) proposed granulite-facies conditions of ≥ 820 °C, ≥ 10 kbar after intrusion. Khmaralite and associated minerals are inferred to have formed by metamorphism of pre-existing pegmatitic Be phases such as beryllian cordierite.

The stable assemblage inferred for no. 2234L(3), khmaralite + sillimanite + surinamite + musgravite + garnet + biotite + rutile, is one of three assemblages found in the surinamite-bearing pegmatites at "Zircon Point" and nearby "Christmas Point" (Fig. 1). The phase relationships illustrated in Figure 1 is a simplification because of the presence of substantial Zn in musgravite. Zinc stabilizes an assemblage in no. 2234L(5) (Grew 1981) not consistent with the array shown: sillimanite + surinamite + musgravite + quartz. Nonetheless, to a first approximation, the phase relations imply that the assemblage musgravite + surinamite + sillimanite saturates khmaralite in Be at the *P* and *T* of metamorphism given that Be is incorporated in khmaralite by the substitution $BeSiAl_{-2}$ (Grew 1981). In contrast, beryllian sapphirine containing 0.6–1.2 wt% BeO from the Musgrave Ranges, Australia, is associated with musgravite, spinel, and biotite, but not surinamite and sillimanite (Wilson and Hudson 1967; Grew and Shearer, unpublished data), and thus would not be expected to be saturated in Be. Another factor favoring Be incorporation could be high Fe^{2+}/Mg ratio in sapphirine and khmaralite (see below).

PHYSICAL PROPERTIES

No cleavage was observed in khmaralite. The luster is vitreous. The hardness is about 7. It is brittle and the fracture is uneven. The color is very dark green; streak is green-gray. The calculated density is 3.61 g/cm^3. In thin section, khmaralite is

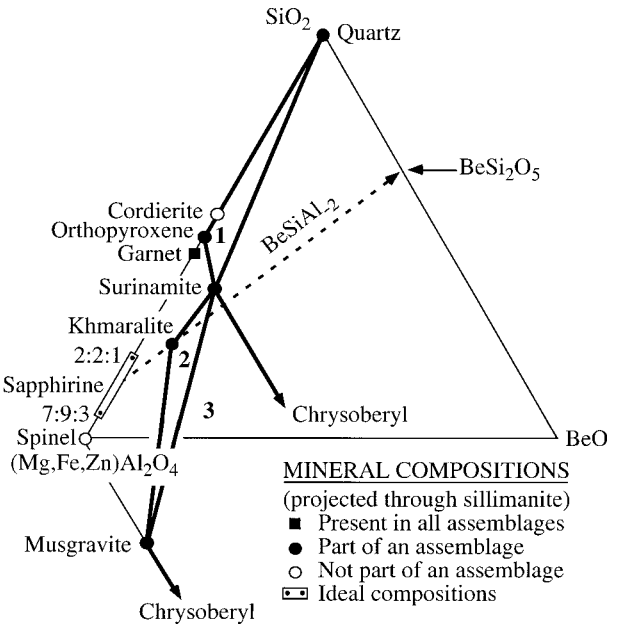

FIGURE 1. Assemblages of Be minerals in pegmatites of Casey Bay (all with sillimanite). The numbered assemblages are identified as follows (Grew 1981, Table 1): (1) no. 2292B, "Christmas Point," (2) no. 2234L(3), "Zircon Point," and (3) no. 2234L(4,5), "Zircon Point." The dashed line marked $BeSiAl_{-2}$ is one of an array of lines converging on the point $BeSi_2O_5$; infinite amount of $BeSiAl_{-2}$ substitution is required to reach this point along any one of these lines.

transparent and biaxial negative. Optical constants measured (method of Bloss 1981; Su 1983, 1998) at λ = 589 nm are α = 1.725(2), β = 1.740(2), γ = 1.741(2), and $2V_{meas}$ = 34.4 (1.8)°, $2V_{calc}$ = 29°; v > r is strong, and $2V_{meas}$ (486 nm) = 49.3(0.8)° and $2V_{meas}$ (656 nm) = 62.6 (0.6)°. The orientation is $\beta \,||\, b$. The pleochroism α = colorless or very light tan, β = blue-green, and γ = deep blue-green. Calculation of the Gladstone-Dale relationship using Eggleton's (1991) constants (for pyroxenes and pyroxenoids where possible; B_2O_3 constant is taken from Mandarino 1981) yields compatibility indices of –0.0007 for a BeO constant of 0.307 and –0.0096 for a BeO constant of 0.236. Both indices are in the "superior" category (Mandarino 1981).

CHEMICAL COMPOSITION

Khmaralite was analyzed for constituents other than Li, Be, and B with an ARL-EMX electron microprobe at UCLA in 1980; operating conditions were 15 kV accelerating voltage, 20 nA sample current (method given in Grew 1980) (Table 1). The three light elements were analyzed in 1982 with an ARL Ion Microprobe Mass Analyzer (IMMA) at the Aerospace Corporation ($^{16}O^-$ beam, method given in Grew et al. 1990) and in 1996 with a Cameca ims 4f (Secondary Ion Mass Spectroscopy or SIMS) operated on the University of New Mexico (UNM) campus by a UNM-Sandia National Laboratories consortium ($^{16}O^-$ beam , method given in Grew et al. 1998). The $^9Be^+$ signal was not corrected for the $^{27}Al^{3+}$ signal in the IMMA data. Assuming that the $^{27}Al^{3+}$ is 5×10^{-5} the intensity of the $^{27}Al^+$ signal (Grew et al. 1990), its contribution would constitute no more than 0.5% of the $^9Be^+$ signal for sapphirine and no more than 0.2% of the $^9Be^+$ signal for the surinamite standard. The SIMS data were obtained at a resolution sufficient to separate the $^9Be^+$ and $^{27}Al^{3+}$ signals. The IMMA and SIMS BeO contents are respectively, 2.56 and 2.47 wt%, which is good agreement given the difference in the instruments and operating conditions.

CRYSTALLOGRAPHY

Electron diffraction and microsocopy

Crystals of khmaralite were extracted from sample no. 2234L(3) (Grew 1981), crushed with an agate pestle and mortar, suspended in butanol, and deposited onto a carbon film supported by a copper grid. Examination in a Philips CM12 transmission electron microscope confirmed the presence of the superstructure originally reported by Christy (1988). Rows of weak extra reflections were present corresponding to a doubling of the **a** axis and all diffraction patterns were indexed on the following unit cell ($P2_1/c$ setting): a = 19.8, b = 14.4, c = 11.2 Å, β = 125° (Fig. 2).

The superstructure was also observed in medium-resolution lattice images of a few crystals viewed along the [001] zone axis. A faint contrast was visible in the thicker regions of the crystals corresponding to a double d_{100} interplanar spacing equal to 16.1 Å (Fig. 2).

Powder X-ray diffraction

The X-ray powder pattern of khmaralite (Table 2) was recorded with a Guinier-Lenné camera using Fe$K\alpha_1$ radiation (λ = 1.93604 Å) and Y_2O_3 as internal standard. The line positions and intensities were measured with a computer-controlled digital film scanner (LS20, KEJ Instruments, Sweden). The powder pattern was completely indexed on a monoclinic unit cell with the parameters listed in Table 2 and with absences consistent with the $P2_1/c$ space group. This unit cell is similar to that determined by Christy (1988) [a = 19.794(8), b = 14.367(5), c = 11.320(3) Å, β = 125.49(4)°], except for an unexplained 0.066 Å difference in the c parameters.

None of the reflections corresponding to the 2×**a** superstructure is visible in the powder X-ray pattern of khmaralite, even after a prolonged exposure time of about three hours. This observation is consistent with the single-crystal X-ray data (see

TABLE 1. Chemical composition of khmaralite

	wt%	Std. Dev.	Range	Standard	Method	Formula*
SiO_2	20.27	0.37	19.7–20.7	Pyrope glass	EMPA†	4.796
Al_2O_3	51.15	0.39	50.4–51.6	Kyanite	EMPA†	14.263
Cr_2O_3	0.01	0.01	0–0.02	Chromite	EMPA†	0.000
Fe_2O_3*	0.70	–	–	calculated	–	0.125
FeO*	9.43	–	–	calculated	–	1.866
FeO*	10.06	0.26	9.6–10.5*	Magnetite	EMPA†	–
MnO	0.01	0.01	0–0.04	Verma garnet	EMPA†	0.000
MgO	15.49	0.20	15.2–15.9	Pyrope glass	EMPA†	5.463
ZnO	0.10	0.09	0–0.2	Zincite	EMPA†	0.000
CaO	0.16	0.03	0.1–0.2	Wollastonite	EMPA†	0.041
K_2O	0.03	0.03	0–0.06	Orthoclase	EMPA†	0.000
Na_2O	0	0	0–0	Jadeite	EMPA†	0.000
Li_2O‡	~0.01	–	~0.01, ~0.01	Spd, Tur‡	IM, SI§	–
BeO	2.51	–	2.47, 2.56	Surinamite	IM, SI§	1.427
B_2O_3	0.05	–	0.05, 0.05	Grandidierite	IM, SI§	0.020
Total ||	99.76					28.000

Note: Modified from Grew (1981) with addition of ion microprobe data.
* Fe was analyzed as Fe^{2+}; FeO and Fe_2O_3 were calculated assuming 28 cations in a formula for 40 O atoms.
† Electron microprobe analyses at 13 points on 4 grains.
‡ Semiquantitative only because standards unsuitable; Spd = spodumene, Tur = lithian tourmaline.
§ IM =ARL ion microprobe mass analyzer (IMMA); SI = Secondary ion mass spectroscopy (SIMS) with the Cameca ims 4f. Stated values are averages of several analyses with each instrument.
|| Does not include Cr_2O_3, FeO (measured), MnO, ZnO, K_2O and Li_2O. In addition, semi-quantitative emission spectrographic analyses gave in wt% Be 0.5–1.0; Ca, Ga 0.1–0.5; B, Co, Ni, V 0.01–0.05; Ba, Cu, Pb, Ta, Sn, Zn <0.01; Li, not detected.

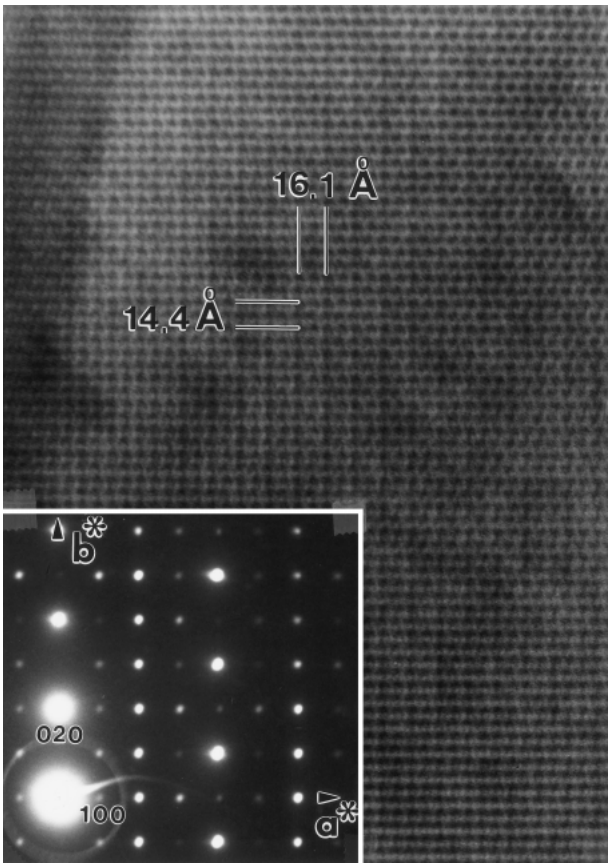

FIGURE 2. TEM lattice image and electron diffraction pattern of khmaralite viewed along the [001] zone-axis. The 2× **a** superstructure is revealed by the weak {*h* odd} reflections and the faint doubling of the d_{100} spacing in the thicker regions of the crystal.

below) showing that the intensity of the strongest super-cell reflection (–7, 8, 6) is only 0.4% of that of the most intense sub-cell reflection (16, 0, 0).

Structure determination by single-crystal X-ray diffraction

A small, irregular, dark-green crystal of khmaralite (220 × 180 × 80 μm³) was selected from sample 2234L(3) (Grew 1981) and mounted on a Siemens diffractometer equipped with a Mo*K*α rotating anode and a SMART area detector (Siemens 1996). To obtain good intensity measurements of the weak superstructure reflections, the X-ray generator was run at 15 kW power and the exposure time for individual frames of the area detector was increased to 60 s. Table 3 summarizes details of the data collection.

The single-crystal X-ray data were indexed on a pseudo-orthogonal monoclinic unit cell with β = 90.9° (other cell parameters are given in Table 3) by using the SAINT program (Siemens 1996). The geometrical relationship between this unit cell and the alternative one with β = 125.5° (corresponding to a simple doubling of the sapphirine-2*M* unit cell; cf. Moore 1969; Higgins and Ribbe 1979b) is illustrated in Figure 3. The superstructure in khmaralite is best described in terms of the doubled (2×**a**) sapphirine unit cell since the **a** axis is the direction of the tetrahedral chains along which the main cation ordering occurs (see below). However, the pseudo-orthogonal unit cell itself was preferred for the structure determination because it was found to lead to fewer inter-parameter correlations during the least-squares refinement cycles.

After correction of the intensity data for absorption using the SADABS program (Sheldrick 1996), the structure refinement was carried out with the SHELXL93 software (Sheldrick 1993). Initially, only a sub-cell structure similar to sapphirine-2*M* was refined in order to determine average cation popula-

TABLE 2. Powder X-ray diffraction pattern of khmaralite

h	*k*	*l*	d_{cal} (Å)	d_{obs}(Å)	I_{obs}	I_{cal}
0	1	1	7.7228	7.7321	6	13
0	2	0	7.1844	7.1859	2	9
2	2	0	5.3620	5.3655	2	2
0	0	2	4.5790	4.5803	8	16
–4	1	2	4.4217	4.4217	3	1
2	3	0	4.1170	4.1150	2	3
–4	2	1	4.0351	4.0336	6	6
0	4	0	3.5922	3.5906	5	8
–4	2	3	3.2654	3.2643	13	22
–6	1	2	3.2162	3.2151	2	4
4	3	0	3.0828	3.0817	7	12
–6	2	2	2.9987	2.9974	5	6
0	1	3	2.9860	2.9852	38	59
2	2	2	2.9620	2.9615	3	6
4	2	1	2.8348	2.8341	30	27
0	4	2	2.8263	2.8260	45	57
–4	1	4	2.7607	2.7598	20	25
0	5	1	2.7419	2.7407	2	2
–6	3	2	2.7174	2.7169	5	7
6	0	0	2.6855	2.6850	5	8
–6	0	4	2.6689	2.6691	3	4
6	1	0	2.6396	2.6408	16	13
–6	1	4	2.6241	2.6240	12	8
–2	1	4	2.5993	2.5990	5	10
0	3	3	2.5743	2.5745	8	10
–4	4	3	2.5657	2.5659	36	40
6	2	0	2.5155	2.5153	8	9
–2	2	4	2.4804	2.4804	4	7
–4	5	2	2.4442	2.4446	100	100
–8	0	2	2.4385	2.4387	44	53
–6	4	2	2.4302	2.4316	2	3
–4	3	4	2.4257	2.4261	6	6
2	4	2	2.4105	2.4111	5	4
0	6	0	2.3948	2.3948	4	6
4	1	2	2.3757	2.3756	15	15
4	4	1	2.3404]	2.3405	43	27]
4	5	0	2.3394			10
–6	3	4	2.3314	2.3312	3	4
–2	3	4	2.3140	2.3138	3	5
0	0	4	2.2895	2.2892	2	1
–8	1	1	2.2346	2.2349	7	5
–8	2	4	2.2108	2.2110	2	2
6	4	0	2.1508	2.1511	3	2
–2	4	4	2.1288	2.1289	3	3
–4	2	5	2.1245]	2.1235	11	5]
0	6	2	2.1221			10
–8	1	5	2.0657	2.0657	5	8
–8	3	1	2.0455	2.0453	3	3
8	0	0	2.0141	2.0140	61	52
–4	5	4	2.0103	2.0106	85	100
0	7	1	2.0030	2.0034	2	3
–8	4	4	1.9510	1.9515	2	2
8	2	0	1.9393	1.9392	3	2
4	6	1	1.8917]	1.8914	29	6]
–4	4	5	1.8910			18
6	0	2	1.8868	1.8874	3	1

Note: The pattern is indexed on the following unit cell: a = 19.800(1), b = 14.369(2), c = 11.254(1) Å, β = 125.53(1)°. The calculated intensities are based on the single-crystal X-ray structure refinement. Note that all the {*hkl*, *h* odd} reflections corresponding to the 2x**a** superstructure have calculated intensities below 1% and none of them is observed.

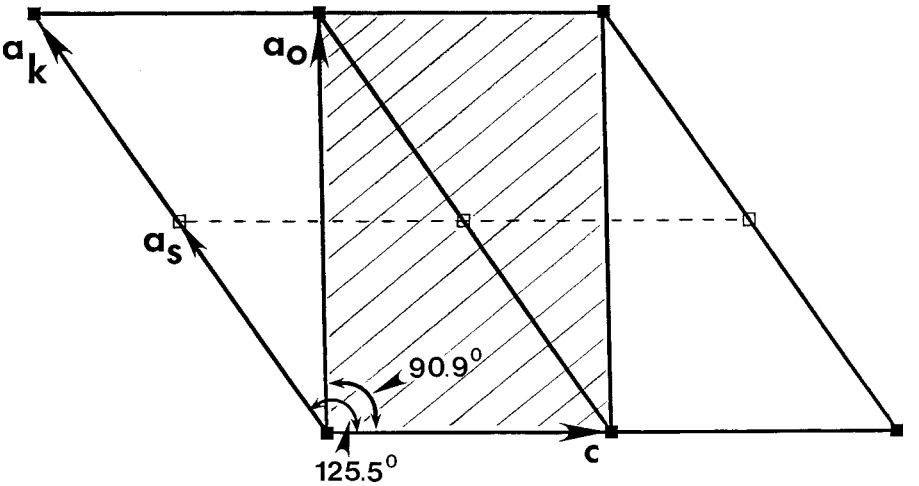

FIGURE 3. Geometrical relationships between the sapphirine-2*M* unit cell (a_s = 9.90 Å, β = 125.5°), the 2×**a** super-cell of khmaralite (a_k = 19.80 Å, β = 125.5°) and the pseudo-orthogonal unit cell (a_o = 16.11 Å, β = 90.9 °) used for the structure refinement of khmaralite. All unit cells have common **b** and **c** axes and correspond to the $P2_1/c$ space group.

TABLE 3. Single-crystal X-ray data collection and structure refinement of khmaralite

Chemical formula	$Mg_{5.46}Fe_{2.00}Al_{14.28}Be_{1.46}Si_{4.80}O_{40}$*
Space group	$P2_1/c$
a (Å)	16.115(1) †
b(Å)	14.371(1)
c (Å)	11.254(1)
β (°)	90.90(1) †
V (Å^3)	2605.98
Z	4
μ (mm^{-1}) (Mo$K\alpha$)	2.14
2θ max (°)	81.89
h_{min}, h_{max}	–28, 27
k_{min}, k_{max}	0, 25
l_{min}, l_{max}	0, 19
Observed reflections	60683 ($I > -3\sigma(I)$)
Independent reflections	14363
Absorption correction	based on equivalent reflections (SADABS software)
T_{min}, T_{max}	0.619, 0.767
R_{int}	0.042 / 0.025 (before/after SADABS correction)
Parameters refined	614 in final anisotropic cycles
Reflections used	14349 (14 omitted in final cycles)
Reflections with $F_o > 4\sigma(F_o)$	10220
Weighting scheme	$[\sigma^2(F_o^2) + w\,P)^2\,]^{-1}$ with P =(max(F_o^2,0)+2F_c^2)/3 , w = 0.057
$R(F)$ ($F_o > 4\sigma(F_o)$)	0.036
$wR(F^2)$ (all)	0.108
$(\Delta\rho)_{min}$ (e.Å^{-3})	–1.82
$(\Delta\rho)_{max}$ (e.Å^{-3})	1.70

* Simplified chemical formula based on 28 cations. The small amounts of Ca and B in the analytical data (0.04 and 0.02 per 40 O atoms; Table 1) have been ignored. The simplified chemical formula implies 1.88 Fe^{2+} + 0.12 Fe^{3+}, in good agreement with the analytical formula.
† Pseudo-orthogonal unit-cell used for the structure refinement (cf. Fig. 3).

tions for the eight octahedral sites and the six tetrahedral sites. After convergence, the structure was expanded into the pseudo-orthogonal supercell, with the same $P2_1/c$ symmetry. The refinement of the atomic coordinates, site occupancies (assuming all sites to be fully occupied) and isotropic displacement parameters of all 16 octahedral (M) sites, 12 tetrahedral (T) sites, and 40 oxygen sites was then undertaken. The refinement is based on a simplified chemical formula, viz., $Mg_{5.46}Fe_{2.00}Al_{14.28}Be_{1.46}Si_{4.80}O_{40}$, in which B is combined with Be and the small amount of Ca is ignored. The assumed stoichiometry of 28 cations and 40 oxygen atoms requires that Fe be present as 1.88 Fe^{2+} + 0.12 Fe^{3+} and the structure refinement indicated that the tetrahedral sites contained a total of 0.07 Fe per forty O atoms. Taking all tetrahedral Fe as Fe^{3+} led to the following coordination formula for khmaralite: $^{[6]}(Mg_{5.46}Al_{8.61}Fe^{2+}_{1.88}Fe^{3+}_{0.05})\,^{[4]}(Al_{5.67}Si_{4.80}Be_{1.46}Fe^{3+}_{0.07})\,O_{40}$. Based on this formula, the occupancies of the individual M and T sites were further refined with the additional constraints of equal U_{eq} parameters for all M sites on one hand and for all T sites on the other. Because it was not possible to simultaneously refine more than two cation occupancies on any given site, the $^{[6]}$(Mg,Al) and $^{[4]}$(Al,Si) occupancies were initially taken as Al only (the majority cations in both types of sites). At this stage, convergence of the $^{[6]}$Fe , $^{[4]}$Be, and $^{[4]}$Fe populations was obtained

with good esd's of 0.3% for all sites. After fixing these populations at their refined values, the $^{[6]}$(Mg/Al) and $^{[4]}$(Al/Si) ratios of individual sites were refined and convergence was again achieved with reasonable esd's of 3% for all sites. It should be pointed out here that the small amount of Fe^{3+} (2–3%) determined for some of the T sites was significant in determining proper Al/Si ratios consistent with their mean <T-O> bond lengths . In the absence of Fe^{3+}, the Al/Si ratios of these sites refined to low values inconsistent with observed <T-O> distances longer than 1.70 Å. The final octahedral and tetrahedral site populations in khmaralite are given in Tables 4a and 4b. In further cycles of refinement, the site occupancies were fixed and the coordinates and displacement parameters of all M, T, and O sites were refined, first isotropically and then anisotropically. The final reliability indices are given in Table 3. The final atomic coordinates and isotropic U_{eq} parameters are listed in Table 5, the anisotropic U_{ij} parameters are listed in Table 6.[1]

TABLE 4a. Octahedral site occupancies and average bond lengths in khmaralite

	%Fe	%Mg	%Al	<M-O> (Å)
M1	4	0 (4)	96 (96)	1.917
M2	2	0 (6)	98 (94)	1.920
M3	7	0 (56)	93 (44)	1.956
M4	24	76 (100)	0 (0)	2.096
M5	18	57 (100)	25 (0)	2.126
M6	21	79 (100)	0 (0)	2.137
M7	3	0 (0)	97 (100)	1.919
M8	3	0 (12)	97 (88)	1.926
M9	7	27 (4)	66 (96)	1.928
M10	10	17 (6)	73 (94)	1.949
M11	15	61 (56)	24 (44)	2.055
M12	17	83 (100)	0 (0)	2.093
M13	28	72 (100)	0 (0)	2.161
M14	25	75 (100)	0 (0)	2.154
M15	4	0 (0)	96 (100)	1.919
M16	4	0 (12)	96 (88)	1.926

Note: The esd's on the Fe populations are 0.3%, those on the Mg and Al populations are 3%. The numbers in parentheses represent the M1-8 site populations in sapphirine-2*M* (Higgins and Ribbe 1979b).

TABLE 4b. Tetrahedral site occupancies and average bond lengths in khmaralite

	%Al	%Si	%Fe	%Be	<T-O> (Å)
T1	73 (92)	27 (8)	–	–	1.745
T2	33 (1)	16 (99)	–	51	1.638
T3	4 (51)	78 (49)	–	18	1.655
T4	38 (92)	59 (8)	–	3	1.690
T5	61 (100)	37 (0)	2	–	1.702
T6	76 (73)	22 (27)	2	–	1.751
T7	61 (92)	39 (8)	–	–	1.724
T8	0 (1)	95 (99)	–	5	1.629
T9	30 (51)	0 (49)	–	70	1.664
T10	96 (92)	4 (8)	–	–	1.753
T11	85 (100)	12 (0)	3	–	1.767
T12	9 (73)	91 (27)	–	–	1.667

Note: The esd's on the Be and Fe populations are 0.3%, those on the Al and Si populations are 3%. The numbers in parentheses represent the T1-6 site populations in sapphirine-2*M* (Higgins and Ribbe 1979b).

[1] For a copy of the table of calculated and observed structure factors, Document item AM-99-028, contact the Business Office of the Mineralogical Society of America (see inside front cover of a recent issue) for price information. Deposit item may also be available on the *American Mineralogist* web site at http://www.minsocam.org.

TABLE 5. Atomic coordinates ($\times 10^5$) and isotropic displacement parameters (in $Å^2$, $\times 10^4$) for khmaralite

Site*	x	y	z	z' †	U_{eq}
M1	6767(2)	15950(2)	–5979(3)	787	53(1)
M2	30694(2)	15904(2)	–31654(3)	–960	53(1)
M3	18813(2)	5663(2)	–18449(3)	363	54(1)
M4	43951(2)	5696(2)	–43855(2)	96	58(1)
M5	7223(2)	36836(2)	–6464(2)	759	55(1)
M6	30409(2)	37321(2)	–31160(2)	–751	57(1)
M7	43740(2)	25938(2)	–43755(3)	–15	55(1)
M8	43783(2)	24859(2)	–18710(3)	25073	54(1)
M9	56946(2)	15861(2)	–55686(3)	1260	55(1)
M10	80404(2)	15344(2)	–82020(3)	–1616	55(1)
M11	68715(2)	5624(2)	–68682(3)	33	56(1)
M12	93494(2)	5719(2)	–93847(2)	–353	57(1)
M13	57726(2)	37211(2)	–56684(2)	1043	61(1)
M14	79912(2)	37061(2)	–80751(2)	–840	60(1)
M15	93696(2)	25841(2)	–93826(3)	–130	54(1)
M16	93620(2)	24922(2)	–68757(3)	24863	53(1)
T1	12523(2)	55322(2)	7500(3)	20023	45(1)
T2	37853(3)	55263(3)	–17448(4)	18801	46(1)
T3	25517(2)	44937(2)	–5142(3)	18798	45(1)
T4	49964(2)	44408(2)	–29784(3)	19965	47(1)
T5	37776(2)	75132(2)	–18975(3)	18814	46(1)
T6	25335(2)	24640(2)	–6537(3)	18734	47(1)
T7	62550(2)	55428(2)	–42714(3)	20405	47(1)
T8	87702(2)	55249(2)	–67401(3)	20375	44(1)
T9	75273(4)	45194(5)	–54963(6)	20180	49(1)
T10	3(2)	44167(2)	19962(3)	19835	46(1)
T11	87801(2)	75577(2)	–68986(3)	20301	46(1)
T12	75220(2)	25148(2)	–56486(3)	20310	47(1)
O1	43926(5)	–25671(5)	–56405(7)	–12478	66(1)
O2	18532(5)	–25032(5)	–31536(7)	–13004	67(1)
O3	6258(4)	5891(5)	5554(6)	11814	54(1)
O4	30918(5)	5977(5)	–19645(7)	11273	76(1)
O5	18201(5)	15655(5)	–7024(7)	11177	77(1)
O6	7843(4)	–16963(5)	–18107(6)	–10264	51(1)
O7	18993(5)	–4900(5)	–7531(7)	11462	71(1)
O8	6767(5)	6083(5)	–17604(7)	–10836	61(1)
O9	44138(5)	–25268(5)	–31211(7)	12926	68(1)
O10	18724(5)	–25433(5)	–5834(7)	12890	68(1)
O11	43859(5)	–46189(5)	–28915(7)	14943	72(1)
O12	19011(5)	–46087(5)	–4654(7)	14357	75(1)
O13	19399(5)	15396(5)	–30292(7)	–10892	65(1)
O14	4996(5)	–16834(5)	5750(6)	10745	46(1)
O15	32622(5)	–35101(5)	–18823(7)	13799	61(1)
O16	6357(5)	–34607(5)	6499(7)	12856	57(1)
O17	43946(5)	–45906(5)	–58271(7)	–14325	89(1)
O18	18583(5)	–46500(5)	–33301(7)	–14718	68(1)
O19	29676(5)	–35167(5)	–43684(7)	–14009	69(1)
O20	6670(5)	–34461(5)	–18930(6)	–12261	54(1)
O21	94132(5)	–25604(5)	–5983(7)	–11851	52(1)
O22	68156(5)	–25199(5)	–80959(7)	–12803	60(1)
O23	56476(5)	5920(5)	–44776(7)	11700	67(1)
O24	81161(5)	5192(5)	–70281(7)	10880	82(1)
O25	68466(5)	16572(5)	–56825(7)	11641	82(1)
O26	57580(4)	–16952(5)	–68162(6)	–10582	49(1)
O27	68734(5)	–5750(5)	–57214(7)	11519	67(1)
O28	56270(5)	6166(5)	–67674(7)	–11404	76(1)
O29	94415(5)	–25161(5)	–81537(7)	12878	50(1)
O30	68465(5)	–25652(5)	–56440(7)	12026	59(1)
O31	93602(4)	–45973(5)	–78993(6)	14609	63(1)
O32	68424(5)	–46186(5)	–54871(7)	13552	82(1)
O33	69073(5)	16136(5)	–80738(7)	–11665	92(1)
O34	54805(5)	–17164(5)	–44298(6)	10507	53(1)
O35	82433(5)	–35166(5)	–68688(7)	13746	54(1)
O36	56172(5)	–34792(5)	–43582(7)	12591	74(1)
O37	93915(5)	–45726(5)	–7569(7)	–13653	68(1)
O38	68573(5)	–46402(5)	–83218(6)	–14645	65(1)
O39	79933(5)	–35256(5)	–93602(7)	–13669	67(1)
O40	56128(5)	–34735(5)	–68979(7)	–12852	64(1)

* The M and T site labeling follows that in sapphirine-2*M* (Higgins and Ribbe, 1979b). The unit cell contains two equivalent sub-cells (M1-8, T1-6 and M9-16, T7-12). The O_n and O_{n+20} sites are equivalent to the O_n sites in sapphirine-2*M*.

† The (x,y,z) coordinates refer to the unit cell with $\beta = 90.9°$ used for the refinement, the (x,y,z' with z' = x+z) coordinates refer to the alternative unit cell with $\beta = 125.5°$ used for the structural description (cf. Fig. 3).

CATION ORDERING IN KHMARALITE

Our structure determination confirms that, as first suggested by Christy (1988), khmaralite represents an ordered derivative of sapphirine-2*M*. The crystal structure of the latter has already been discussed in detail by Moore (1968, 1969), Higgins and Ribbe (1979a, 1979b), Merlino (1973, 1980), Christy and Putnis (1988), Barbier and Hyde (1988), and by Christy (1989) and, therefore, the present paper describes only the cation distribution peculiar to khmaralite. The site occupancies are given in Tables 4a and 4b and illustrated in Figures 4 and 5; the bond distances are listed in Table 7 together with selected bond angles and polyhedral edge lengths. Note that Figure 5 is, in fact, a projection along c' = [103] = 27.475 Å with respect to the $\beta = 125.5°$ axial setting, the axis perpendicular to the closest packed layers of the khmaralite structure. The layer separation in this 12-layer repeat (4.ccc.) is h = c'/12 = 2.290 Å, equal to the typical separation in sapphirine, spinel, kyanite, etc. For example, in the six-layer repeat (2.ccc.) of spinel, Al_2MgO_4, $h = \sqrt{3}a/6 = 2.339$ Å.

Much of the difference between sapphirine-2*M* and khmaralite is in the tetrahedral sites; the octahedral ordering in khmaralite is similar to that in sapphirine-2*M* and there are only small differences between the two M1-8 and M9-16 sub-cells (Table 4a). The contrast in Fe-Mg-Al octahedral occupancies is most marked for M3 (7-0-93) and M11 (15-61-24). Not surprisingly, the larger Mg^{2+} and Fe^{2+} cations are concentrated in the octahedral sites with fewer shared edges and inherently larger volumes, such as M5, M6, M13, and M14 (Figs. 4 and 5). This results in a pronounced Fe^{2+}-Al^{3+} avoidance similar to that observed in Fe-rich sapphirine-1*A* (Merlino 1980). Presumably, the minor amount of octahedral Fe^{3+} in khmaralite (0.05 Fe^{3+} per 40 O atoms) is accommodated in the Al-rich sites. The highest Fe-contents (21–28%) are found for the M4, M6, M13, and M14 sites which are the only ones to share two corners with the Be-rich T2 or T9 tetrahedral sites (see below and Figs. 4 and 5). This particular Fe ordering can be understood in terms of bond-valence sum requirements around the shared oxygen atoms as follows: for a given M-O bond distance, the Fe-O bond valence is larger than the Mg-O bond valence due to the difference in bond-valence parameters, viz., 1.734 and 1.693 for Fe^{2+}-O and Mg-O bonds, respectively (Brese and O'Keeffe 1991); consequently, for an oxygen atom already bonded to two Be-rich tetrahedral sites (with low bond-valence contributions from the Be-O bonds), a proper bond-valence sum is expected to require a higher Fe/Mg ratio for the octahedral site(s) also sharing that oxygen. Therefore, the distribution of octahedral Fe in khmaralite appears to be driven, in part at least, by the presence of tetrahedral Be. It differs from that in the aenigmatite-group mineral serendibite, $\sim(Ca,Na)_2(Mg,Fe)_3(Al,Fe)_{4.5}B_{1.5}Si_3O_{20}$, in which no significant Fe ordering was found (Van Derveer et al. 1993). One factor contributing to this difference is occupancy of the larger M8 and M9 sites in serendibite by Ca and Na only. By analogy, the small amount of Ca in khmaralite (0.04 Ca per 40 O atoms; Table 1) is presumed to occupy the corresponding M5, M6, M13, and M14 sites.

Conversely, a high Fe/Mg ratio probably creates a more favorable environment for Be incorporation. Khmaralite is richer in Fe^{2+} than any of the 21 sapphirine compositions reviewed by Deer et al. (1978) and than all but one of the 23 natural sapphirine compositions reported by Christy (1989).

The difference in tetrahedral distribution between sapphirine-2*M* and khmaralite is primarily due to the presence of tetrahedral Be in the latter, which results in distinct cation ordering between the two T1-6 and T7-12 sub-cells (Table 4b). The strongest contribution to the superstructure comes from Al-Si-Be ordering on the T2 (33-16-51%) vs. T8 (0-95-5%) and T3 (4-78-18%) vs. T9 (30-0-70%) sites, i.e., Be is the major constituent only at two of the four tetrahedral sites which share corners with three other tetrahedra. These two sites—T2 and T9—are not commensurate with the sub-cell and therefore contribute to the superstructure. Overall, the tetrahedral cation distribution in khmaralite also involves significant Be/Si and Al/Si ordering. For instance, the Be-rich T9 site shares corners with Si-rich T8 and T12 sites and, in turn, the T8 site shares corners with the Al-rich T10 and T11 sites (Figs. 4 and 5). Such a distribution, as well as a strong preference for Be/Al mixing over Be/Si mixing, appear to be required to satisfy the bonding requirements of the

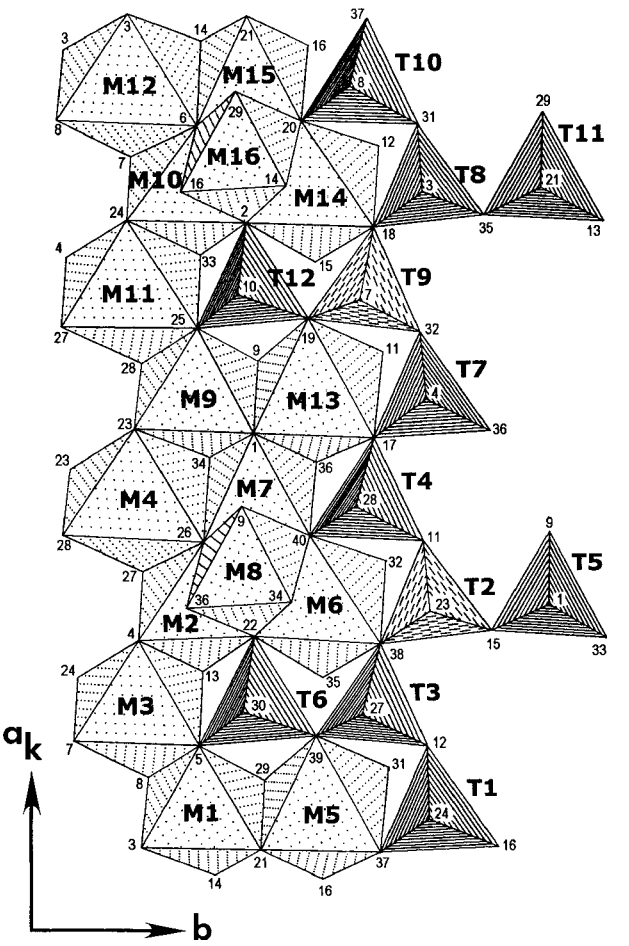

FIGURE 4. Part of the khmaralite structure projected on to the (001) plane showing the (M1-8, T1-6) and (M9-16, T7-12) sapphirine-like sub-cells alternating along the a_k axis (cf. Fig. 3). Be is concentrated in the non-equivalent T2 and T9 sites. The numbers at the corners of the polyhedra refer to the oxygen positions (cf. Table 5).

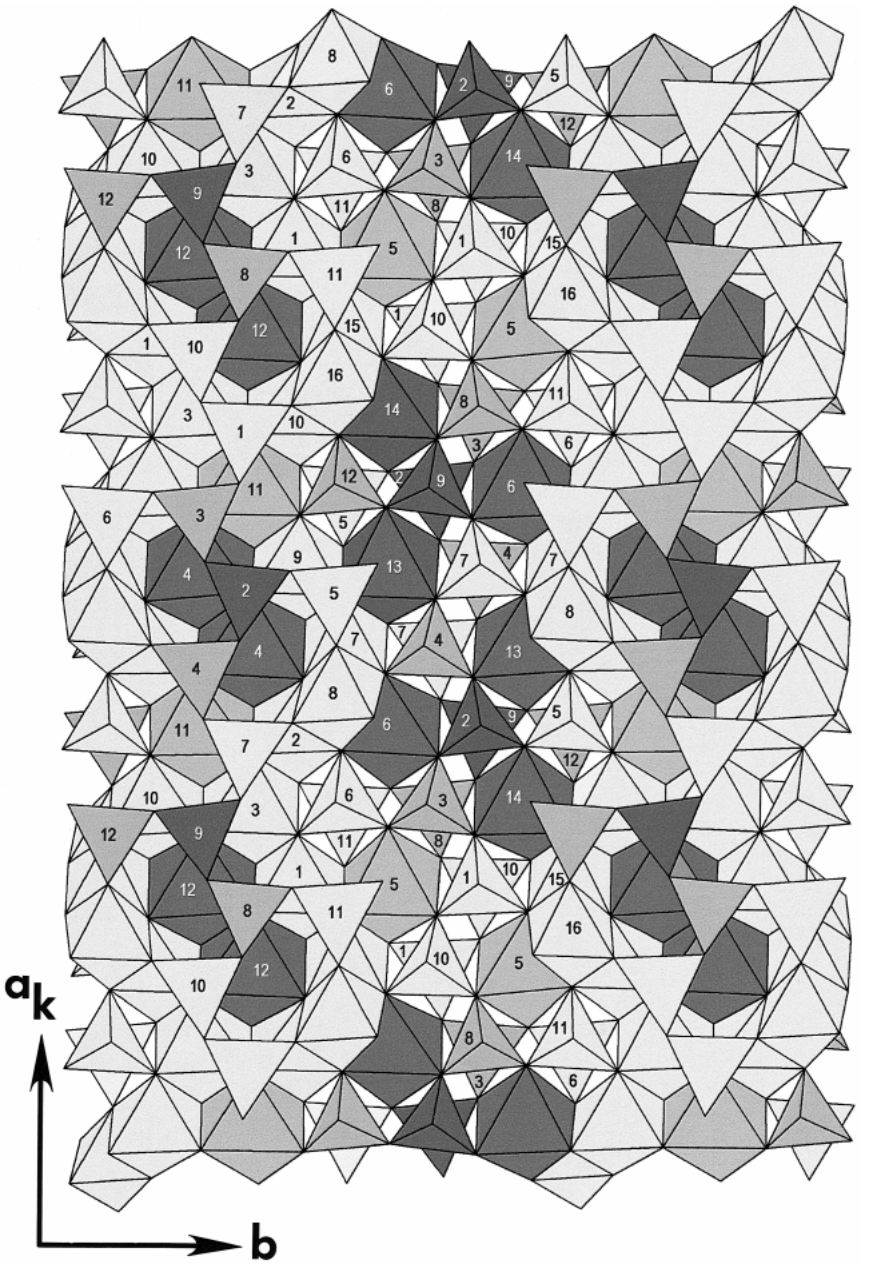

FIGURE 5. Cation distribution in the khmaralite structure. The numbers refer to the octahedral and tetrahedral site labels (cf. Fig. 4 and Table 5). The dark-, medium- and light-gray tetrahedra are Be-, Si-, and Al-rich respectively (cf. Table 4b). The dark-gray octahedra have the highest Fe-contents (and no Al), the medium-gray octahedra have high (Fe + Mg)-contents (with some Al) and the light-gray octahedra are Al-rich (cf. Table 4a). A clustering of Be-rich T sites and Fe-rich M sites is apparent.

bridging O atoms by minimizing the number of Be-O-Be and Be-O-Al linkages. The inherent underbonding of these bridging O atoms is expected to make such linkages less likely than Be-O-Si or Al-O-Si linkages. An analogous preference for Be/B mixing over Be/Si mixing became apparent in a new refinement of hyalotekite, $(Ba,Pb,K)_4(Ca,Y)_2Si_8(B,Be)_2(Si,B)_2O_{28}F$, a tectosilicate related to scapolite (Christy et al. 1998).

To a first approximation, the sequence Al-Si-Al in sapphirine is replaced by the sequence Si-Be-Si in khmaralite; i.e., Be replaces Si on two sites and Si replaces Al on four adjacent sites, resulting in an indirect replacement of Al by Be by the coupled substitution Be + Si = 2Al. Electron and ion microprobe analyses show that this substitution describes the overall variation in Si, Al, and Be between Be-free sapphirine, beryllian

TABLE 7. Bond lengths (Å) and selected polyhedral edge lengths* (Å) and bond angles (°) in khmaralite

M1-O5	1.849(1)		M6-O22	2.222(1)		M12-O14	2.101(1)		T4-O11	1.675(1)	
M1-O14	1.900(1)		Mean	2.137		M12-O6	2.116(1)		T4-O28	1.689(1)	
M1-O8	1.929(1)					M12-O3	2.127(1)		T4-O17	1.691(1)	
M1-O29	1.937(1)		M7-O34	1.861(1)		M12-O8	2.131(1)		T4-O40	1.706(1)	
M1-O21	1.940(1)		M7-O26	1.876(1)		Mean	2.093		Mean	1.690	
M1-O3	1.945(1)		M7-O36	1.911(1)							
Mean	1.917		M7-O40	1.911(1)		M13-O19	2.051(1)		T5-O33	1.671(1)	
			M7-O30	1.968(1)		M13-O11	2.084(1)		T5-O15	1.689(1)	
O14-O21*	2.515(1)	81.81(4)	M7-O1	1.988(1)		M13-O17	2.117(1)		T5-O1	1.716(1)	
O14-O29*	2.542(1)	82.97(4)	Mean	1.919		M13-O9	2.209(1)		T5-O9	1.731(1)	
O5-O8*	2.576(1)	85.95(4)				M13-O1	2.237(1)		Mean	1.702	
O3-O8*	2.609(1)	84.65(4)	M8-O34	1.870(1)		M13-O36	2.267(1)				
O3-O14*	2.703(1)	89.33(4)	M8-O26	1.874(1)		Mean	2.161		T6-O5	1.729(1)	
O8-O29	2.750(1)	90.66(4)	M8-O22	1.924(1)					T6-O39	1.746(1)	
O21-O29*	2.752(1)	90.40(4)	M8-O9	1.947(1)		M14-O15	2.039(1)		T6-O30	1.757(1)	
O5-O29	2.752(1)	93.22(4)	M8-O36	1.959(1)		M14-O18	2.095(1)		T6-O22	1.770(1)	
O3-O5	2.786(1)	94.46(4)	M8-O40	1.984(1)		M14-O12	2.102(1)		Mean	1.751	
O8-O14	2.800(1)	93.96(4)	Mean	1.926		M14-O20	2.195(1)				
O3-O21	2.834(1)	93.67(4)				M14-O2	2.225(1)		T7-O32	1.692(1)	
O5-O21	2.869(1)	98.39(4)	M9-O25	1.866(1)		M14-O10	2.265(1)		T7-O17	1.727(1)	
Mean	2.707	89.95	M9-O23	1.886(1)		Mean	2.154		T7-O4	1.733(1)	
			M9-O34	1.903(1)					T7-O36	1.743(1)	
O3-O29	3.870(1)	170.69(4)	M9-O28	1.941(1)		M15-O6	1.872(1)		Mean	1.724	
O8-O21	3.866(1)	175.48(4)	M9-O1	1.966(1)		M15-O14	1.879(1)				
O5-O14	3.747(1)	176.18(4)	M9-O9	2.006(1)		M15-O20	1.898(1)		O17-O32	2.747(1)	106.89(4)
			Mean	1.928		M15-O16	1.903(1)		O4-O32	2.777(1)	108.34(4)
M2-O13	1.830(1)					M15-O21	1.962(1)		O17-O36	2.782(1)	106.57(4)
M2-O26	1.896(1)		O1-O34*	2.520(1)	81.27(4)	M15-O10	2.002(1)		O4-O17	2.838(1)	110.22(4)
M2-O27	1.926(1)		O9-O34*	2.561(1)	81.83(4)	Mean	1.919		O4-O36	2.865(1)	111.01(4)
M2-O30	1.945(1)		O23-O28*	2.577(1)	84.63(4)				O32-O36	2.876(1)	113.71(4)
M2-O22	1.956(1)		O23-O34*	2.713(1)	91.43(4)	M16-O6	1.881(1)		Mean	2.814	109.46
M2-O4	1.965(1)		O9-O25	2.723(1)	89.30(4)	M16-O14	1.894(1)				
Mean	1.920		O25-O28*	2.741(1)	92.10(4)	M16-O29	1.928(1)		T8-O18	1.617(1)	
			O9-O28	2.749(1)	88.26(4)	M16-O16	1.944(1)		T8-O35	1.623(1)	
M3-O5	1.931(1)		O28-O34	2.752(1)	91.43(4)	M16-O20	1.949(1)		T8-O31	1.636(1)	
M3-O13	1.935(1)		O23-O25	2.828(1)	97.84(4)	M16-O2	1.959(1)		T8-O3	1.641(1)	
M3-O8	1.946(1)		O1-O25	2.830(1)	95.18(4)	Mean	1.926		Mean	1.629	
M3-O7	1.953(1)		O1-O9*	2.835(1)	91.09(4)						
M3-O4	1.958(1)		O1-O23	2.842(1)	95.08(4)	T1-O37	1.726(1)		T9-O19	1.653(1)	
M3-O24	2.010(1)		Mean	2.723	89.95	T1-O12	1.746(1)		T9-O32	1.659(1)	
Mean	1.956					T1-O24	1.749(1)		T9-O7	1.670(1)	
			O9-O23	3.878(1)	170.08(4)	T1-O16	1.758(1)		T9-O18	1.674(1)	
M4-O23	2.023(1)		O25-O34	3.755(1)	170.35(4)	Mean	1.745		Mean	1.664	
M4-O27	2.050(1)		O1-O28	3.899(1)	172.69(4)						
M4-O23	2.104(1)					O12-O37	2.776(1)	106.15(4)	T10-O37	1.732(1)	
M4-O26	2.125(1)		M10-O33	1.837(1)		O12-O24	2.813(1)	107.15(4)	T10-O31	1.758(1)	
M4-O34	2.131(1)		M10-O6	1.908(1)		O16-O37	2.829(1)	108.60(4)	T10-O8	1.761(1)	
M4-O28	2.143(1)		M10-O7	1.910(1)		O24-O37	2.834(1)	109.27(4)	T10-O20	1.764(1)	
Mean	2.096		M10-O24	1.971(1)		O16-O24	2.916(1)	112.49(4)	Mean	1.753	
			M10-O10	1.999(1)		O12-O16	2.921(1)	112.95(4)			
M5-O37	2.042(1)		M10-O2	2.070(1)		Mean	2.848	109.43	T11-O13	1.741(1)	
M5-O39	2.082(1)		Mean	1.949					T11-O35	1.770(1)	
M5-O31	2.101(1)					T2-O15	1.627(1)		T11-O21	1.771(1)	
M5-O21	2.151(1)		M11-O28	2.012(1)		T2-O11	1.638(1)		T11-O29	1.786(1)	
M5-O29	2.167(1)		M11-O24	2.017(1)		T2-O23	1.642(1)		Mean	1.767	
M5-O16	2.212(1)		M11-O33	2.032(1)		T2-O38	1.644(1)				
Mean	2.126		M11-O25	2.064(1)		Mean	1.638		T12-O19	1.642(1)	
			M11-O27	2.083(1)					T12-O25	1.644(1)	
M6-O32	2.034(1)		M11-O4	2.124(1)		T3-O38	1.645(1)		T12-O10	1.685(1)	
M6-O38	2.083(1)		Mean	2.055		T3-O39	1.650(1)		T12-O2	1.695(1)	
M6-O35	2.092(1)					T3-O27	1.662(1)		Mean	1.667	
M6-O30	2.191(1)		M12-O7	2.024(1)		T3-O12	1.664(1)				
M6-O40	2.201(1)		M12-O3	2.059(1)		Mean	1.655				

* Asterisks indicate shared octahedral edges.

sapphirine, and khmaralite (Grew 1981; Grew and Shearer 1999 and unpublished data). An analogous situation is found for boron in the kornerupine group, in which B appears to replace Al due to a coupling of B for Si substitution on one site (T3) and Si for Al substitution on an adjacent site (T2, e.g., Klaska and Grew 1981). Although Be is incorporated on a site that is Si-rich in sapphirine, little or no Si remains on the Be-rich sites in khmaralite; instead, the balance is made up largely by Al. That Be shares sites with Al instead of Si is known to hold true for natural, highly ordered beryllian cordierite (e.g., Armbruster 1986) as well as for a synthetic, partially disordered cordierite-like phase $Mg_2[Al_2BeSi_6O_{18}]$ isostructural with beryl (Hölscher and Schreyer 1989).

The tetrahedral cation distribution in khmaralite shows simi-

larities with that in the related Be-bearing mineral surinamite, $^{[6]}(Mg_3Al_3)^{[4]}(AlBeSi_3)O_{16}$. In the latter, Al, Si, and Be are completely ordered, Be-O-Al linkages are absent, and Be occupies a topologically unique site sharing corners with three other (SiO_4) tetrahedra (Moore and Araki 1983). Four topologically similar sites occur in khmaralite (T2, T3, T8, and T9) and these are split into two Be-rich sites (T2, T9) and two Si-rich sites (T3, T8) in such a way as to favor the formation of Be-O-Si linkages (Fig. 5). The different degrees of tetrahedral ordering in the surinamite and khmaralite structures are probably related to the different topologies of their tetrahedral chains, with the more symmetrical sapphirine-like chains in khmaralite precluding a completely ordered distribution. Indeed, a similar difference in tetrahedral ordering has also been observed in the structures of the synthetic surinamite and sapphirine analogues recently characterized in the MgO-Ga_2O_3-GeO_2 system (Barbier 1998).

In contrast to khmaralite, a disordered Be/Si distribution (with Al-Si-Be proportions of 10-40-50% on T1 and 0-50-50% on the adjacent T4 site) has been determined in the structure of "makarochkinite," which also contains sapphirine-like tetrahedral chains, but no evidence of a superstructure (Yakubovich et al. 1990). Due to this unexpected Be distribution and because "makarochkinite" is reported to have 1.60 Be per 28 cations (vs. 1.43 Be in khmaralite), we are now carrying out our own refinement of its crystal structure. An initial examination by electron diffraction has confirmed the absence of superstructure in "makarochkinite," but a preliminary single-crystal X-ray refinement suggests significant differences in the site occupancies as compared to those determined previously (Yakubovich et al. 1990).

The Be distribution in khmaralite also differs markedly from the B distribution in the aenigmatite-group mineral, serendibite. In this case, B is accommodated in two adjacent tetrahedral sites, 98% in T4 and 65% in T1 (Van Derveer et al. 1993), equivalent to the T2/T8 and T3/T9 sites of khmaralite. Superstructure reflections were not reported in serendibite. The difference between the B and Be distributions in these minerals undoubtedly reflects the greater stability of B-O-B linkages over Be-O-Be linkages.

Finally, it can be noted that the small amount of tetrahedral Fe^{3+} in khmaralite is exclusively located at the T5, T6, and T11 Al-rich sites forming the wings of the tetrahedral chains (Fig. 4). This result contradicts Steffen et al. (1984), who concluded that Fe^{3+} is randomly distributed among the tetrahedral sites on the basis of a Mössbauer spectroscopic study of natural and synthetic sapphirines.

DISTINGUISHING KHMARALITE FROM SAPPHIRINE–2*M*

The critical distinctions between khmaralite and sapphirine-2*M* are (1) the presence of the 2×**a** superstructure and (2) the predominance of Be at one tetrahedral site. Electron and ion microprobe data on sapphirine containing from 0.6 to 1.7 wt% BeO suggest that there is a continuous solid solution between Be-free sapphirine of composition $(Mg,Fe)_{7.5}(Al,Fe)_{17}Si_{3.5}O_{40}$ and khmaralite (Grew and Shearer 1999 and unpublished data). A simple 50% rule to divide the sapphirine-khmaralite pseudobinary solid solution series is not practical because the amount of Be on a given site and the resulting superstructure depend on the extent of cation order as well as total amount of Be. Appearance of the 2×**a** superstructure is undoubtedly a function of Be content, but we do not know how much Be is necessary to evince it, nor do we know how much total Be is necessary in order for one site to be predominantly occupied by Be.

Thus, distinguishing the two minerals using microprobe analyses, powder X-ray patterns, and optical properties, which are the most readily obtained data, would not give an unequivocal identification in most cases. The two minerals cannot be distinguished on the basis of their optical properties, because the effect of Be is overshadowed by the effect of Fe substitution for Mg and Al. Nonetheless, a crystal structure refinement may not be necessary to establish the presence of khmaralite. A sapphirine-like mineral containing 2 wt% or more BeO, which is roughly equivalent to 1.1 or more Be per 40 oxygen atoms, and 19–20 wt% SiO2, is most likely khmaralite. Confirming the presence of the superstructure by electron diffraction, which is more sensitive than X-ray diffraction to such features and more easily carried out, would probably clinch the identification because the superstructure would be expected to develop only if Be were ordered on certain sites.

ACKNOWLEGMENTS

J.B.'s research was supported by a research grant from the Canadian Natural Sciences and Engineering Research Council. E.S.G.'s research was supported by U.S. National Science Foundation grant OPP-9813569. We thank N. Marquez, C. Shearer, and M. Wiedenbeck for assistance in obtaining the ion probe data and J. Britten (McMaster University) for the collection of the single-crystal X-ray data.

REFERENCES CITED

Armbruster, T. (1986) Role of Na in the structure of low-cordierite: A single-crystal X-ray study. American Mineralogist, 71, 746–757.

Barbier, J. (1998) Crystal structures of sapphirine and surinamite analogues in the MgO-Ga_2O_3-GeO_2 system. European Journal of Mineralogy, 10, 1283–1293.

Barbier, J. and Hyde, B.G. (1988) Structure of sapphirine: its relation to the spinel, clinopyroxene and β-gallia structures. Acta Crystallographica, B44, 373–377.

Blose, F.D. (1981) The Spindle Stage: Principles and Practice. Cambridge University Press. 340 p.

Brese, N.E. and O'Keeffe, M. (1991) Bond-valence parameters for solids. Acta Crystallographica, B47, 192–197.

Christy, A.G. (1988) A new 2**c** superstructure in beryllian sapphirine from Casey Bay, Enderby Land, Antarctica. American Mineralogist, 73, 1134-1137.

——(1989) The effect of composition, temperature and pressure on the stability of the 1Tc and 2M polytypes of sapphirine. Contributions to Mineralogy and Petrology, 103, 203–215.

Christy, A.G. and Putnis, A. (1988) Planar and line defects in the sapphirine polytypes. Physics and Chemistry of Minerals, 15, 548–558.

Christy, A.G., Grew, E.S., Mayo, S.C. , Yates, M.G., and Belakovskiy, D.I. (1998) Hyalotekite, $(Ba,Pb,K)_4(Ca,Y)_2Si_8(B,Be)_2(Si,B)_2O_{28}F$, a tectosilicate related to scapolite: new structure refinement, phase transitions and a short-range ordered 3*b* superstructure. Mineralogical Magazine, 62, 77–92.

de Roever, E.M.F., Lattard, D., and Schreyer, W. (1981) Surinamite: a beryllium-bearing mineral. Contributions to Mineralogy and Petrology, 76, 472–473.

Deer, W.A., Howie, R.A., and Zussman, J. (1978) Rock-Forming Minerals, vol 2A. Single-Chain silicates, 2nd ed. Longman, London

Eggleton, R.A. (1991) Gladstone-Dale constants for the major elements in silicates: coordination number, polarizability, and the Lorentz-Lorentz relation. Canadian Mineralogist, 29, 525–532.

Grauch, R.I., Lindahl, I., Evans, H.T., Jr, Burt, D.M., Fitzpatrick, J.J., Foord, E.E., Graff, P.-R., and Hysingjord, J. (1994) Høgtuvaite, a new beryllian member of the aenigmatite group from Norway, with new X-ray data on aenigmatite. Canadian Mineralogist, 32, 439–448.

Grew, E.S. (1980) Sapphirine + quartz association from Archean rocks in Enderby Land, Antarctica. American Mineralogist, 65, 821–836.

——(1981) Surinamite, taaffeite, and beryllian sapphirine from pegmatites in granulite-facies rocks of Casey Bay, Enderby Land, Antarctica. American Mineralogist., 66, 1022–1033.

——(1998) Boron and Beryllium Minerals in Granulite-facies Pegmatites and Implications of Beryllium Pegmatites for the Origin and Evolution of the Archean

Napier Complex of East Antarctica. Memoirs of the National Institute of Polar Research, Special Issue, 53, 74–92.

Grew, E.S. and Shearer, C.K. (1999) Beryllium and boron in the Napier Complex, Enderby Land, East Antarctica. In Skinner, D.N.B., ed., 8th International Symposium on Antarctic Earth Sciences, Programme & Abstracts, Victoria University of Wellington, Wellington, New Zealand, 5–9 July, 1999, p.128.

Grew, E.S., Chernosky, J.V., Werding, G., Abraham, K., Marquez, N., and Hinthorne, J.R. (1990) Chemistry of kornerupine and associated minerals, a wet chemical, ion microprobe, and x-ray study emphasizing Li, Be, B and F contents. Journal of Petrology, 31, 1025–1070.

Grew, E.S., Yates, M.G., Huijsmans, J.P.P., McGee, J.J., Shearer, C.K., Wiedenbeck, M., and Rouse, R.C. (1998) Werdingite, a borosilicate new to granitic pegmatites. Canadian Mineralogist, 36, 399-414.

Higgins, J.B. and Ribbe, P.H. (1979a) Sapphirine I: Crystal chemical contributions. Contributions to Mineralogy and Petrology, 68, 349–356.

——(1979b) Sapphirine II: A neutron and X-ray diffraction study of $(Mg\text{-}Al)^{VI}$ and $(Al\text{-}Si)^{IV}$ ordering in monoclinic sapphirine. Contributions to Mineralogy and Petrology, 68, 357–368.

Hölscher, A. and Schreyer, W. (1989) A new synthetic hexagonal BeMg-cordierite, $Mg_2[Al_2BeSi_6O_{18}]$, and its relationship to Mg-cordierite. European Journal of Mineralogy, 1, 21–37.

Hölscher, A., Schreyer, W., and Lattard, D. (1986) High-pressure, high-temperature stability of surinamite in the system $MgO\text{-}BeO\text{-}Al_2O_3\text{-}SiO_2\text{-}H_2O$. Contributions to Mineralogy and Petrology, 92, 113–127.

Klaska, R. and Grew, E.S. (1991) The crystal structure of boron-free kornerupine: Conditions favoring the incorporation of variable amounts of B through $^{[4]}B \leftrightarrow {}^{[4]}Si$ substitution in kornerupine. American Mineralogist, 76, 1824–1835.

Mandarino, J.A. (1981) The Gladstone-Dale relationship: Part IV. The compatibility concept and its application. Canadian Mineralogist, 19, 441–450.

Merlino, S. (1973) Polymorphism in sapphirine. Contributions to Mineralogy and Petrology, 41, 23–29.

——(1980) Crystal structure of sapphirine-1Tc. Zeitschrift für Kristallographie, 151, 91–100.

Moore, P.B. (1968) Crystal structure of sapphirine. Nature, 218, 81–82.

——(1969) The crystal structure of sapphirine. American Mineralogist, 54, 31–49.

——(1978) Welshite, $Ca_2Mg_4Fe^{3+}Sb^{5+}O_2[Si_4Be_2O_{18}]$, a new member of the aenigmatite group. Mineralogical Magazine, 42, 129–132.

Moore, P.B. and Araki, T. (1983) Surinamite, ca. $Mg_3Al_4Si_3BeO_{16}$: its crystal structure and relation to sapphirine, *ca*. $Mg_{2.8}Al_{7.2}Si_{1.2}O_{16}$. American Mineralogist, 68, 804–810.

Polyakov, V.O., Cherepivskaya, G.Ye., and Shcherbakova, Ye.P. (1986) Makarochkinite—a new beryllosilicate. In New and little-studied minerals and mineral associations of the Urals. Sverdlovsk, Ural'skiy Nauchnyy Tsentr Akademii Nauk SSSR, p. 108–110 (in Russian).

Sheldrick, G.M. (1993) SHELXL93, program for the refinement of crystal structures. University of Göttingen, Germany.

——(1996) SADABS, Siemens area detector absorption correction software. University of Göttingen, Germany.

Siemens (1996) SMART and SAINT, area detector control and integration software. Release 4.05. Siemens Analytical X-ray Instruments Inc., Madison, Wisconsin.

Steffen, G., Seifert, F., and Amthauer, G. (1984) Ferric iron in sapphirine: a Mössbauer spectroscopic study. American Mineralogist, 69, 339–348.

Su, S.C. (1993) Determination of refractive index of solids by using dispersion staining method: An analytical approach. In G.W. Baily and C.L. Rieder, Eds., Proceedings of 51st Annual Meeting of the Microscopy Society of America, 456–457.

——(1998) Dispersion staining: Principles, analytical relationships and practical applications to the determination of refractive index. The Microscope, 46, 123–146.

Van Derveer, D.G., Swihart, G.H., Sen Gupta, P.K., and Grew, E.S. (1993) Cation occupancies in serendibite: A crystal structure study. American Mineralogist, 78, 195–203.

Wilson, A.F and Hudson, D.R. (1967) The discovery of beryllium-bearing sapphirine in the granulites of the Musgrave Ranges (Central Australia). Chemical Geology, 2, 209–215.

Yakubovich, O.V., Malinovskii, Yu.A., and Polyakov, V.O. (1990) Crystal structure of makarochkinite. Soviet Physics Crystallography, 35, 818–822

MANUSCRIPT RECEIVED NOVEMBER 16, 1998
MANUSCRIPT ACCEPTED JUNE 18, 1999
PAPER HANDLED BY GILBERTO ARTIOLI